Eur Biophys J (2012) 41:139–145
DOI 10.1007/s00249-011-0765-5

ORIGINAL PAPER

EBSA
Biophysics in Europe

Adhesion and stress relaxation forces between melanoma and cerebral endothelial cells

Attila G. Végh · Csilla Fazakas · Krisztina Nagy · Imola Wilhelm · Judit Molnár · István A. Krizbai · Zsolt Szegletes · György Váró

Received: 11 August 2011 / Revised: 6 October 2011 / Accepted: 11 October 2011 / Published online: 30 October 2011

Abstract Mechanical parameters play a crucial role in proper cellular functions. This article examines the process of the appearance and breaking of adhesion forces during contact between the confluent cerebral endothelial cell layer and a melanoma cell attached to a tipless cantilever. This adhesion is the initial phase of melanoma transmigration through the endothelial cell layer. Taking the force measurement, if the contact was prolonged for several seconds, a decrease in the load force was observed, which corresponds to stress relaxation of the cells. The dependence of adhesion force and stress relaxation on dwell time showed a saturation-like behavior. These stress relaxation curves could be fitted with the sum of two exponentials, suggesting that two independent processes take place simultaneously. The breakup of the adhesion during the retraction of the cantilever with the attached melanoma cell is not continuous but shows jumps. Between living endothelial and melanoma cells, a minimum jump size of about 20 pN could be determined. The minimum jump is independent of the dwell time and load force. It seems to be the elementary binding force between these two cell types. In case of fixed endothelial cells, the adhesion force was strongly decreased and the jumps disappeared, whereas the stress relaxation did not show considerable change upon fixation.

Keywords Atomic force microscopy · Cell elasticity · Endothelium · Cell–cell interaction · Blood-brain barrier

A. G. Végh · C. Fazakas · K. Nagy · I. Wilhelm · J. Molnár · I. A. Krizbai · Z. Szegletes · G. Váró (✉)
Institute of Biophysics, Biological Research Centre of the Hungarian Academy of Sciences, 6726 Szeged, Hungary
e-mail: varo@brc.hu

Introduction

Since the invention of the atomic force microscope (AFM) in 1986 (Binnig et al. 1986), the instrument has evolved into a high-resolution imaging tool capable of determining the micro-mechanical properties of samples, such as the local elasticity and viscosity of the studied object (Santos and Castanho 2004; Vinckier and Semenza 1998; Willemsen et al. 1999). These properties are increasingly being used in the characterization of different biological samples (Ando 2003). Proper morphology and elasticity are essential for multicellular structures. Alterations in cell mechanics induced by various factors can lead to improper cell or even tissue function (Panorchan et al. 2011; Moreno-Flores et al. 2010a; Zhang et al. 2009). Understanding the rules of single cell and intercellular mechanics could open new insights into cellular processes, including the response to different stress factors or cell-cell interactions (Moreno-Flores et al. 2010b; Rabinovich et al. 2005).

Micro-mechanical properties are determined by force measurement with AFM. The curve resulting from the tip approaching and pushing the sample surface with a load force indents the sample, characterized by the local elasticity of the probed object (Dimitriadis et al. 2002; Fritz et al. 1997; Sen et al. 2005). The retracting branch characterizes the adhesion force appearing between the probe and sample (Eastman and Zhu 1996; Puech et al. 2006; Sen et al. 2005). Adhesion forces can be measured between the sample and a surface modified tip also, or by binding a functional group or even a monitoring cell to the cantilever (Berger et al. 1995; Eastman and Zhu 1996). To study cell–cell interactions, a technique was developed using a cell bound to the AFM cantilever as the probe during the measurement (Zhang et al. 2006). It was shown that the cadherin-mediated cell-cell interaction has a minimal binding force in the range of 50 pN (Panorchan et al. 2011; Zhang et al. 2009). By acting on the cells, a stress

appears that relaxes in time. The stress relaxation curve depends on the elasticity and viscosity of the cell, as has been discussed previously (Moreno-Flores et al. 2010a, b).

A large variety of cells has been studied with AFM: bacterial cells (Miclea et al. 2010), epithelial cells (Rabinovich et al. 2005), platelets (Radmacher et al. 1996), and endothelial cells (Bálint et al. 2007; Oberleithner et al. 2003; Végh et al. 2011). Some cancerous cells, such as melanoma cells, were also studied with AFM by imaging and measuring their elastic properties (Tomankova et al. 2007; Klymenko et al. 2009). Although endothelial cells have been intensively studied, fewer data are available on cerebral micro-capillary endothelial cells forming the blood-brain barrier. The cerebral endothelial cells are strongly interconnected by tight and adherens junction proteins localized at their apical plasma membrane. These constitute the blood-brain barrier, which protects the brain from harmful external chemicals circulating in the blood (Wilhelm et al. 2007).

They present unique characteristics compared to other endothelial cells as they play a key role in maintaining homeostasis of the central nervous system. They are continuously exposed to strong external mechanical influences. Some chemicals entering the blood stream can affect the mechanical properties of the endothelial cells (Bálint et al. 2007; Wilhelm et al. 2007). A fast-growing amount of data is available nowadays describing the effect of drugs on living cells (Ehrhardt et al. 2004; Hunziker et al. 2002; Hillebrand et al. 2006; Oberleithner et al. 2003).

Melanoma cells play a key role in the appearance of tumor, and by metastasis they form secondary tumors even in the brain, transmigrating the blood-brain barrier. Several aspects of these cells were studied with AFM, such as the photodynamic effect and cell-cell adhesion (Puech et al. 2006; Tomankova et al. 2007).

In this study we investigated the mechanical properties of human cerebral endothelial cells, such as elasticity and viscosity, and their dependence on the external conditions when a probing cantilever has a murine melanoma skin cancer cell at the tip. Measuring the cell-cell interaction between endothelial and melanoma cells could help to understand how the blood-brain barrier is penetrated by melanoma cells during pathological conditions, since the initial and crucial part of melanoma cell transmigration over the blood-brain barrier is its adhesion to endothelial cells.

Materials and methods

Cell culture

B16/F10 murine melanoma cells were kept in RPMI medium (Sigma) supplemented with 5% FBS (Lonza) and Glutamax. The hCMEC/D3 human cerebral endothelial cells (shortly D3) were grown on rat tail collagen-coated dishes in EBM-2 medium (Lonza) supplemented with EGM-2 Bullet Kit (Lonza) and 2.5% FBS (Sigma) (Wilhelm et al. 2007, 2008). Fixed cells were produced by incubating the endothelial cells with 4% paraformaldehyde solution for 30 min and washed with PBS prior imaging.

AFM

All measurements were carried out with an Asylum MFP-3D head mounted on an Axiovert 200 microscope and Molecular Force Probe Controller (Asylum Research, Santa Barbara, CA), using the MFP-3D Xop driver program written in Igor Pro software (version 6.2.2, Wavemetrics, Lake Oswego, OR). For single cell measurements silicon nitride rectangular cantilevers with "V"-shaped tips (Olympus, Optical Co. Ltd., Tokyo, Japan) and for cell-cell adhesion measurements tipless cantilevers were used (MikroMasch, Tallinn, Estonia). The spring constant was determined by thermal calibration (Hutter and Bechhoefer 1993), resulting in 0.03 N/m in both cases, while their resonant frequency in liquid was 7 and 10 kHz, respectively.

For adhesion decomposition, we developed a homemade MATLAB routine that counts and averages the rupture forces, basically the level differences on the retracting curve. Every step-like feature was counted if the difference was larger than the noise level, which usually was considered twofold the standard deviation from the last 50 points at the end of the curve, roughly around 8–9 pN. The routine simply counts how many such events had taken place in a single adhesion force and finally averages their sizes.

Force measurements

The individual melanoma cells were attached to a surface-activated tipless cantilever using a Concanavalin-A (Con A)—mediated linkage (Zhang et al. 2006). With the help of the Axiovert 200 microscope, the cantilever was gently lowered onto a melanoma cell for approximately 1 s to attach the cell to its end. After each set of measurements, the position of the melanoma cells was checked with the microscope, and no considerable changes were observed. All measurements were carried out in Leibovitz medium (Sigma) at 32°C within 3 h. According to our observations and to the literature, the cells preserve their viability during this period (Pesen and Hoh 2005). All force measurements were carried out with the same loading rate of 2 μm/s.

Results and discussion

The force measurement with AFM has great importance in determining the micromechanical properties of biological

objects. There are two representation modes of the measured signal: as a function of the distance of the tip from the probe (Fig. 1a) and as a function of time (Fig. 1b). In the distance-dependent representation two features can be clearly seen: the rise of the approaching curve, determining the indentation of the sample, and the negative force on the retracting branch yielding the adhesion force. The time-dependent representation shows two extra features: the dwell time and the stress relaxation curve. The dwell time is the time period until the tip is in contact with the sample. Stress relaxation is the decrease of the load force during the dwell time. It appears in all cases when the load force is applied for finite dwell time to an elastic sample.

On Fig. 2 three characteristic parts of the force curves are presented under different measuring conditions. Practically neither stress relaxation nor adhesion was observed between the hard tip and petri dish (curves T-P). It behaves like a hard surface with no indentation, and the slope of the load is very steep. Probing the living confluent endothelial cell layer (curves T-E) with a hard tip, the surface appears to be very soft. A large stress relaxation appears, but there is only a very small adhesion force, almost at the limit of noise. When instead of a hard tip a melanoma cell is the probe over the living confluent endothelial cell layer

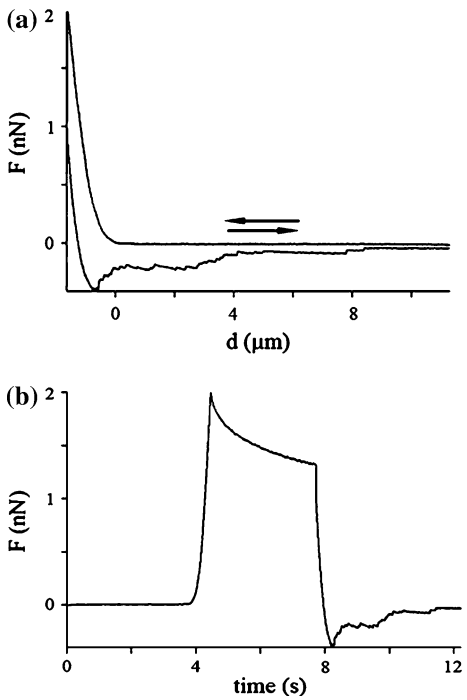

Fig. 1 Force measurement effectuated with a melanoma cell bound to a tipless cantilever on a living confluent endothelial cell layer. The measurement is shown in two representations: force as a function of distance (**a**) and force as a function of measurement time (**b**). While the load force and the adhesion are visible in both representations, the dwell time and the stress relaxations are visible only on the time-dependent representation

(curves M-E), the contact surface seems similarly soft as in the previous case. Both the stress relaxation and the adhesion force have a large amplitude. During the breaking of the adhesion force, characteristic jumps appear on the retrace. If the melanoma probes a fixed confluent endothelial cell layer (curves M-F), the slope of the load force and the stress relaxation have intermediate values, while the adhesion curve is small, featureless, and smooth.

Adhesion force dependence on dwell time was measured at different load forces. Between the melanoma "tip" and the cell-free surface of the petri dish, there is a small adhesion (Fig. 3a). Changing the load force or dwell time, the change in adhesion is within the error. In the case of a confluent living endothelial cell layer monitored with a melanoma cell, the adhesion as a function of dwell time shows saturation-like behavior (Fig. 3b). It seems that there is a limited amount of adhesion binding at a given load force. Increasing the load, the monitoring cell is pushed closer to the cell layer, and the binding force increases. This increase might be due to an increase in the number of the binding sites or increase in the individual binding forces. On the fixed cell layer, the adhesion force is much weaker (Fig. 3c).

In the case of stress relaxation force as a function of dwell time, the three studied surfaces showed a very similar behavior (Fig. 4a–c). The cell-free surface cannot be distinguished from the living or fixed cell-covered surfaces, suggesting that the melanoma cell has the dominant role in this phenomenon.

The adhesion force measured on living cells showed jumps during breaking up of the contact in the retreat phase of the force curve. Although the jumps were randomly distributed along the force curves, the reproducibility of the total adhesion amplitude and both the number and amplitude of the jumps is very good. These jumps correspond to the rupture of binding between the melanoma cell and endothelial cell covered surface. With the custom-developed MATLAB protocol, the curves were analyzed by searching for the smallest jump and enumerating them. The number of the jumps showed a saturation-like increase as a function of dwell time (Fig. 5a), while the jump size was constant within the error (Fig. 5b), giving an average value of the minimal jump size of about 20 $\pm$ 5 pN. The jumps are smaller on fixed cells. Analyzing the histogram, with the jump frequency as a function of jump size, the living endothelial cells show a clear maximum at 20 pN (Fig. 6a). A value close to this had been measured by others on cadherin-mediated cell-cell adhesion (Panorchan et al. 2011; Zhang et al. 2009). The maximum jump frequency of the fixed cells is shifted to 10 pN (Fig. 6b), which is the size of the measurement noise. These prove that the adhesion between the two cells was altered by fixation.

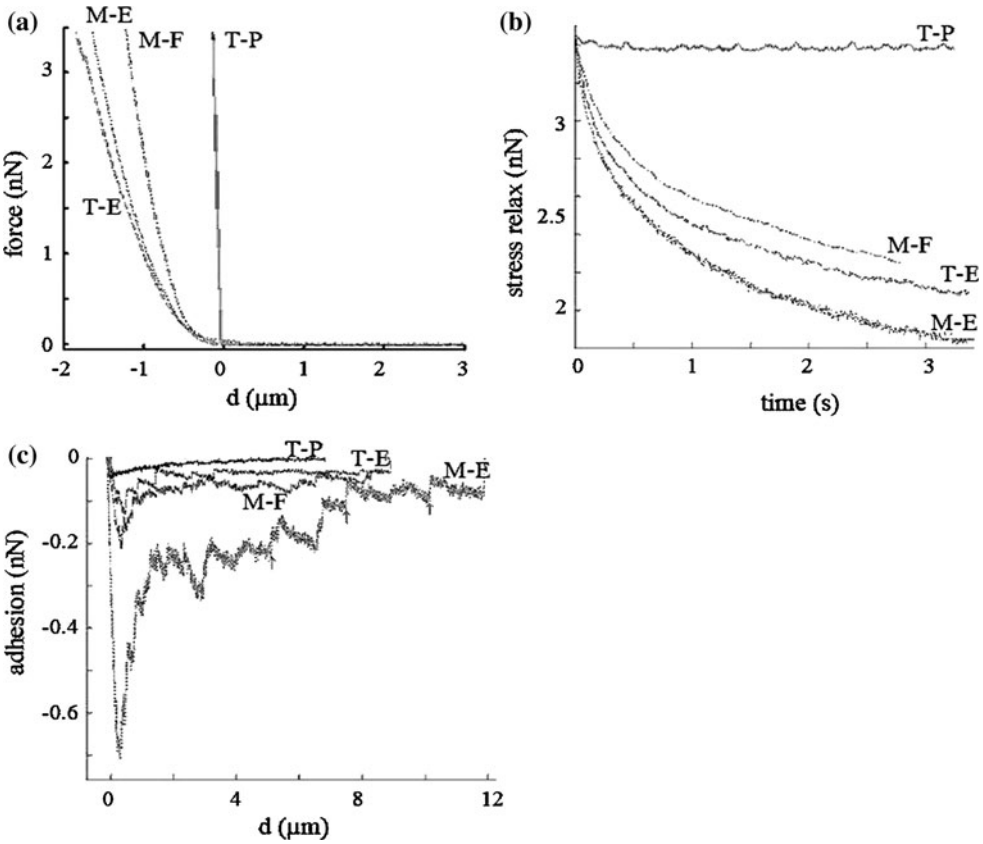

Fig. 2 Comparison of the rise of the load force (**a**), the stress relaxation (**b**), and the adhesion force (**c**). The force was measured on a petri dish with a hard tip (T-P), on a living confluent endothelial cell layer with a hard tip (T-E), on a living confluent endothelial cell layer with a melanoma cell bound to a tipless cantilever (M-E), and on a fixed confluent endothelial cell layer with a melanoma cell bound to a tipless cantilever (M-F)

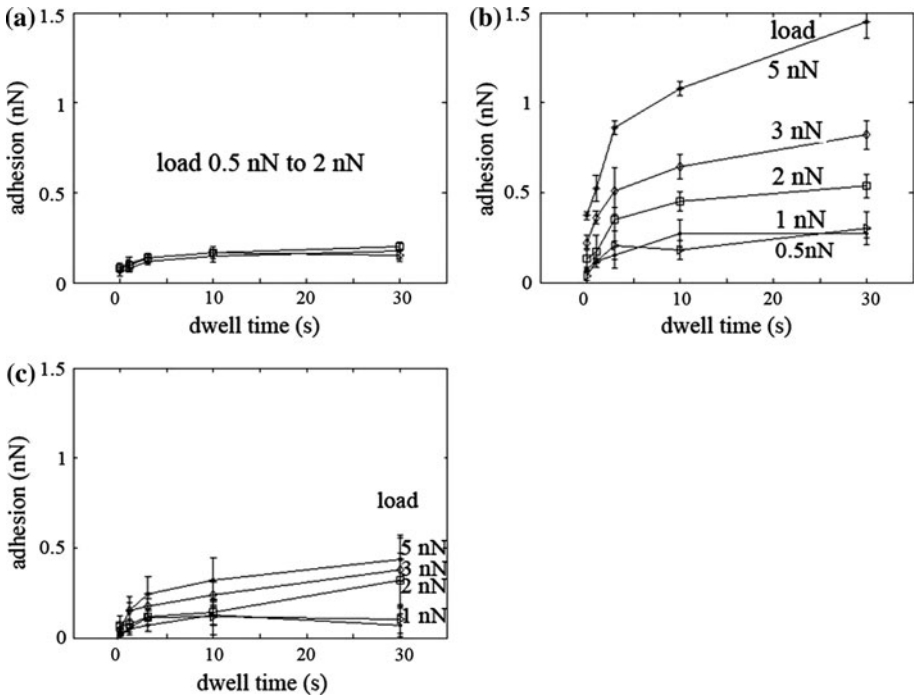

Fig. 3 Change in adhesion as a function of dwell time under constant load. The measurements were effectuated with a melanoma cell bound to a tipless cantilever on a petri dish (**a**), living confluent endothelial cell layer (**b**), and fixed endothelial cell layer (**c**)

Stress relaxation curves were fitted with two exponentials as described by others (Moreno-Flores et al. 2010a, b). The lifetime of the exponentials was weakly dependent on the load force (not shown) as has also been reported for breast cancer cells (Moreno-Flores et al. 2010b). Presented as a function of dwell time, the lifetimes of both the fast and slow components showed a weak, almost linear dependency (Fig. 7a, b), whereas the amplitude in both cases showed

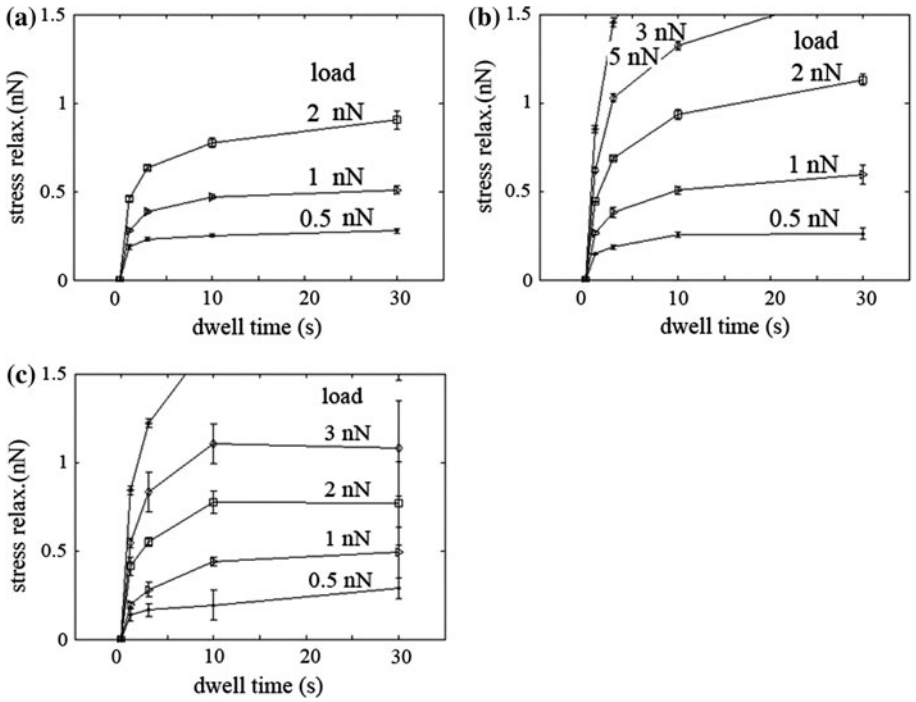

Fig. 4 Change in the stress relaxation force as a function of dwell time under constant load. The measurements were effectuated with a melanoma cell bound to a tipless cantilever on a petri dish (**a**), living confluent endothelial cell layer (**b**), and fixed endothelial cell layer (**c**)

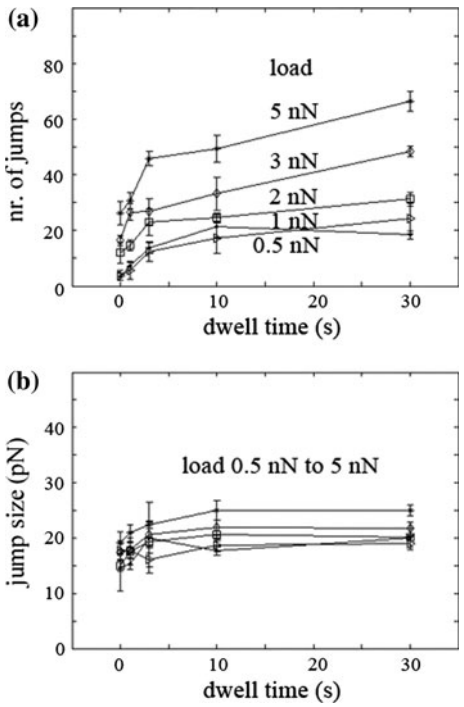

Fig. 5 Number of the jumps (**a**) and the size of the jumps (**b**) when the adhesion breaks between a melanoma cell and living confluent endothelial cell layer

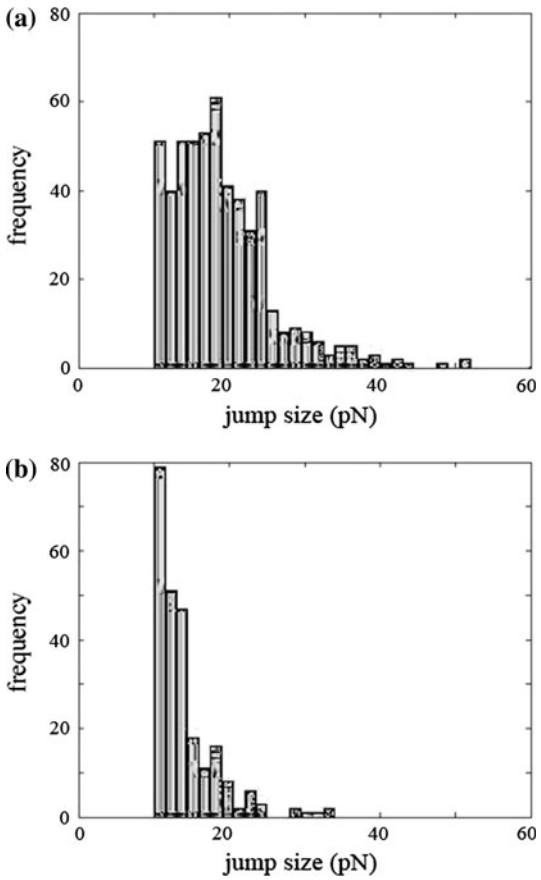

Fig. 6 The histogram of the jump frequency as a function of jump size measured at 2 nN load on living endothelial cells (**a**) and fixed endothelial cells (**b**)

saturation-like behavior (Fig. 7c, d). The slow component saturated within 3 s, much faster than the fast one. The lifetimes are determined by the elasticity and viscosity of both the monitoring melanoma and monitored endothelial cells.

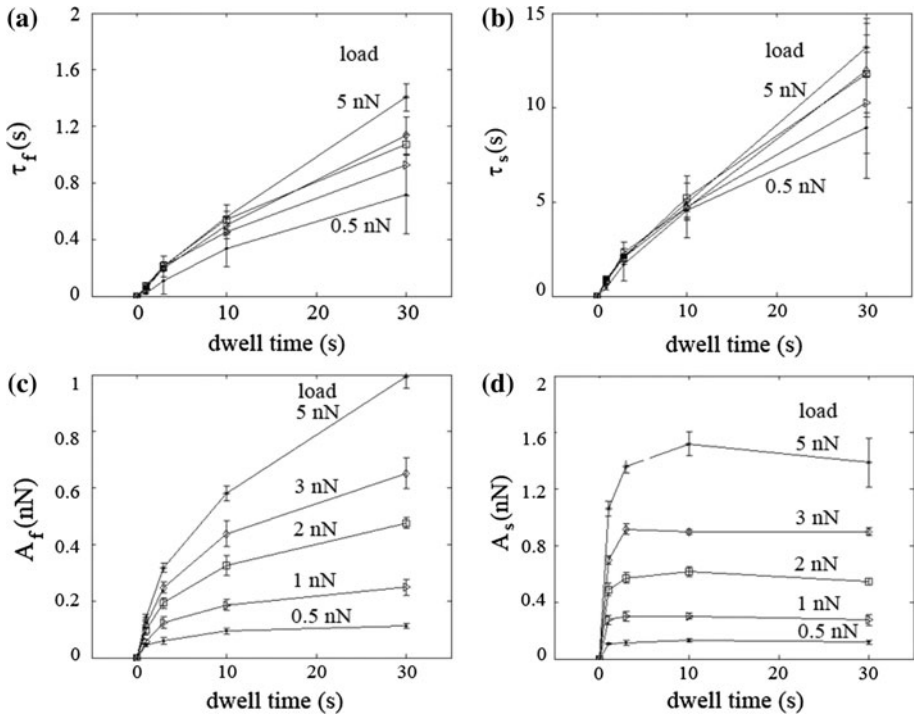

Fig. 7 The dependence of the lifetime and amplitude on the dwell time of the stress relaxation curve measured between a melanoma cell and living confluent endothelial cell layer was fitted with two exponentials. **a** and **c** show the components of the fast exponentials. **b** and **d** present the components of the slow exponential

Conclusion

Two features of force spectroscopy were studied, adhesion force and stress relaxation. Their dependence from the load or the dwell time characterized the interaction among the monitored surface, the endothelial cell layer, and the monitoring melanoma cell. The adhesion force could be decomposed to small elementary jumps, having the size of about 20 pN. This seems to be the strength of one adhesion bond. The dependence of the adhesion force on the load and dwell time suggests that during the contact of the two cells much elementary binding appears, adding up in the adhesion force. The adhesion of the melanoma cell on the fixed cell layer decreased drastically, suggesting that the access to the endothelial binding sites is blocked.

The stress relaxation curve could be fitted with two exponentials, which are determined by the visco-elastic properties of the two objects taking part in the measurement. The amplitude of the slow component saturates within 3 s when the amplitude of the fast component still rises. The different behaviors of the two exponentials suggest that they belong to different phenomena happening in the cells. The stress relaxation did not depend strongly on the state of the cells, whether they were living or fixed. From the above-mentioned observations, it can be concluded that adhesion is more suitable to follow the changes occurring inside or between the cells. By monitoring these mechanical parameters of the cells, information can be collected about their health state.

The direct measurement of the strong binding between melanoma cells and living endothelial cells and the decrease of the binding to fixed cells reflects that a specific interaction takes place between the two cell types. This specific interaction could be the initial step in the transmigration process of the melanoma cells through the confluent endothelial cell layer for penetrating the blood-brain barrier. To clarify the nature of this process, more investigations are needed.

Acknowledgments This work was supported by the National Science Fund of Hungary OTKA K 81180 and Austrian-Hungarian Joint Grant AT-4/2009.

References

Ando T (2003) Atomic force microscope: application to life science. Seikagaku 74:1329–1342

Bálint Z, Krizbai I, Wilhelm I, Farks AE, Párducz Á, Szegletes Z, Váró G (2007) Changes induced by hyperosmotic mannitol in cerebral endothelial cells: an atomic force microscopic study. Eur Biophys J Biophys Lett 36:113–120

Berger CEH, Vanderwerf KO, Kooyman RPH, de Groot B, Greve J (1995) Functional group imagin by adhesion AF applied to lipid monolayer. Langmuir 11:4188–4192

Binnig G, Quate CF, Gerber C (1986) Atomic force microscope. Phys Rev Lett 56:930–933

Dimitriadis EK, Horkay F, Maresca J, Kachar B, Chadwick RS (2002) Determination of elastic moduli of thin layers of soft material using the atomic force microscope. Biophys J 82:2798–2810

Eastman T, Zhu DM (1996) Adhesion forces between surface-modified AFM tips and a mica surface. Langmuir 12:2859–2862

Ehrhardt C, Kneuer C, Bakowsky U (2004) Selectins: an emerging target for drug delivery. Adv Drug Deliv Rev 56:527–549

Fritz J, Anselmetti D, Jarchow J, FernandezBusquets X (1997) Probing single biomolecules with atomic force microscopy. J Struct Biol 119:165–171

Hillebrand U, Hausberg M, Stock C, Shahin V, Nikova D, Riethmuller C, Kliche K, Ludwig T, Schillers H, Schneider SW, Oberleithner H (2006) 17 beta-estradiol increases volume, apical surface and elasticity of human endothelium mediated by Na+/H+ exchange. Cardiovasc Res 69:916–924

Hunziker PR, Stolz M, Aebi U (2002) Nanotechnology in medicine: moving from the bench to the bedside. Chimia 56:520–526

Hutter JL, Bechhoefer J (1993) Calibration of atomic-force microscope tips. Rev Sci Instrum 64:1868–1873

Klymenko O, Wiltowska-Zuber J, Lekka M, Kwiatek WM (2009) Ennergy dissipation in the AFM elasticity measurements. Acta Phys Polonica A 115:548–553

Miclea PS, Péter M, Végh GA, Cinege G, Kiss E, Váró G, Horváth I, Dusha I (2010) Atypical transcriptional regulation and role of a new toxin-antitoxin-like module and its effect on the lipid composition of *Bradyrhizobium japonicum*. Mol Plant Microbe Interact 23:638–650

Moreno-Flores S, Benitez R, Vivanco Md, Toca-Herrera JL (2010a) Stress relaxation microscopy: imaging local stress in cells. J Biomech 43:349–354

Moreno-Flores S, Benitez R, Vivanco Md, Toca-Herrera JL (2010b) Stress relaxation and creep on living cells with the atomic force microscope: a means to calculate elastic moduli and viscosities of cell components. Nanotechnology 21:1–8

Oberleithner H, Schneider SW, Albermann L, Hillebrand U, Ludwig T, Riethmuller C, Shahin V, Schafer C, Schillers H (2003) Endothelial cell swelling by aldosterone. J Membr Biol 196:163–172

Panorchan P, Thompson MS, Davis KJ, Tseng Y, Kanstantopoulos K, Wirtz D (2011) Single-molecule analysis of cadherin-mediated cell–cell adhesion. J Cell Sci 119:66–74

Pesen D, Hoh JH (2005) Micromechanical architecture of the endothelial cell cortex. Biophys J 88:670–679

Puech PH, Poole K, Knebel D, Muller DJ (2006) A new technical approach to quantify cell–cell adhesion forces by AFM. Ultramicroscopy 106:637–644

Rabinovich Y, Esayanur M, Daosukho S, Byer K, El Shall H, Khan S (2005) Atomic force microscopy measurement of the elastic properties of the kidney epithelial cells. J Colloid Interf Sci 285:125–135

Radmacher M, Fritz M, Kacher CM, Cleveland JP, Hansma PK (1996) Measuring the viscoelastic properties of human platlets with the atomic force microscope. Biophys J 70:556–567

Santos NC, Castanho MARB (2004) An overview of the biophysical applications of atomic force microscopy. Biophys Chem 107:133–149

Sen S, Subramanian S, Discher DE (2005) Indentation and adhesive probing of a cell membrane with AFM: theoretical model and experiments. Biophys J 89:3203–3213

Tomankova K, Kolarova H, Vujtek M, Bajgar R (2007) Photodynamic effect on melanoma cells investigated by atomic force microscopy. Gen Physiol Biophys 26:200–206

Végh GA, Fazakas C, Nagy K, Wilhelm I, Krizbai IA, Nagyőszi P, Szegletes Z, Váró G (2011) Spatial and temporal dependence of the cerebral endothelial cells elasticity. J Mol Recognit l24:422–428

Vinckier A, Semenza G (1998) Measuring elasticity of biological materials by atomic force microscopy. Febs Lett 430:12–16

Wilhelm I, Farkas A, Nagyőszi P, Váró G, Bálint Z, Végh GA, Couraud PO, Romero I, Weksler B, Krizbai I (2007) Regulation of cerebral endothelial cell morphology by extracellular calcium. Phys Med Biol 52:6261–6274

Wilhelm I, Nagyőszi P, Farks AE, Couraud PO, Romero I, Weksler B, Fazakas C, Dung NTK, Bottka S, Bauer H, Krizbai IA (2008) Hyperosmotic stress induces Axl activation and cleavage in cerebral endothelial cells. J Neurochem 107:116–126

Willemsen OH, Snel MME, van Noort SJT, van der Werf KO, de Grooth BG, Figdor CG, Greve J (1999) Optimization of adhesion mode atomic force microscopy resolves individual molecules in topography and adhesion. Ultramicroscopy 80:133–144

Zhang XH, Wojcikiewicz EP, Moy VT (2006) Dynamic adhesion of T lymphocytes to endothelial cells revealed by atomic force microscopy. Exp Biol Med 231:1306–1312

Zhang Y, Sivasankar S, Nelson WJ, Chu S (2009) Resolving cadherin interactions and binding cooperativity at the single-molecule level. Proc Natl Acad Sci USA 106:109–114